Sensors & Transducers, Vol. 247, Issue 8, December 2020, pp. 25-32

www.sensorsportal.com

Sensors & Transducers

Published by IFSA Publishing, S. L., 2020
http://www.sensorsportal.com

Fabrication Steps for a POF-WDM Key-Element

[1] M. Haupt, [2] U. H. P. Fischer and [2] Sebastian Höll

[1] Jade University of Applied Sciences, Friedrich-Paffrath-Str. 101, 26389 Wilhelmshaven, Germany

[2] Harz University of Applied Sciences, Friedrichstr. 57-59, 38855 Wernigerode, Germany

[1] Tel.: + 49 4421 985 2625, fax: +49 4421 985 2304

E-mail: matthias.haupt@jade-hs.de

Received: 6 November 2020 /Accepted: 10 December 2020 /Published: 31 December 2020

Abstract: Optical simulation software based on the ray tracing method offers easy and fast results in imaging optics. This method can also be applied in other fields of light propagation, e.g. non-imaging optics. In this paper a miniature spectrometer designed and developed by means of ray tracing will be discussed. Compared to the classical optical design, requirements for optimal design of this element differ particularly with regard to the spatial separation of the different wavelengths and the complete transmission of light to achieve the best signal-to-noise ratio.

The basis of the presented element is a Rowland spectrometer. But for the complete guidance of light that emerges the entrance split the design of this element has to be changed fundamentally, especially when a high numerical aperture of the light beam is taken into account. A monolithic approach is presented with a blazed grating based on an aspheric mirror to suppress most of the aberrations. The grating is analyzed for different diffraction orders and the best possible efficiency. On the exit of this element the light must be guided into different photo diodes with different effective areas. In general, the element should be designed in a way that it can be produced with a mass production technology like injection molding in order to offer a reasonable price. The paper will describe the development of this miniature spectrometer step by step by means of ray tracing simulations.

Keywords: WDM, Polymer Optical Fibers, Multiplexing, Raytracing, Rowland Spectrometer.

1. Introduction

1.1. Advantages of Polymer Optical Fibers

Polymer Optical Fibers (POFs) offer many advantages compared to alternate data communication solutions such as glass fibers, copper cables and wireless communication systems. In comparison with glass fibers, POFs offer easy and cost-efficient processing and are more flexible for plug interconnections. POFs can be passed with smaller radius of curvature and without any mechanical disruption because of the larger diameter compared to glass fibers.

The advantage of using glass fibers is their low attenuation, which is below 0,3 dB/km in the infrared range. In comparison, POF can only provide acceptable attenuation in the visible spectrum from 400 nm up to 700 nm, see Fig. 1. The attenuation has its minimum with about 85 dB/km at approximately 570 nm. For this reason, POF can only be efficiently used for short distance communication up to 100 m and the disadvantage of the larger core diameter is higher mode dispersion.

The use of copper as communication medium is technically outdated, but still the standard for short distance communication. In comparison, POF offers lower weight and space. Another reason is the

nonexistent susceptibility to any kind of electromagnetic interference [1-3].

Wireless communication is afflicted with two main disadvantages. The electromagnetic fields can disturb each other and probably other electronic devices. Additionally, wireless communication technologies provide almost no safeguards against unwarranted eavesdropping by third parties, which makes this technology unsuitable for the secure transmission of volatile and sensitive business information.

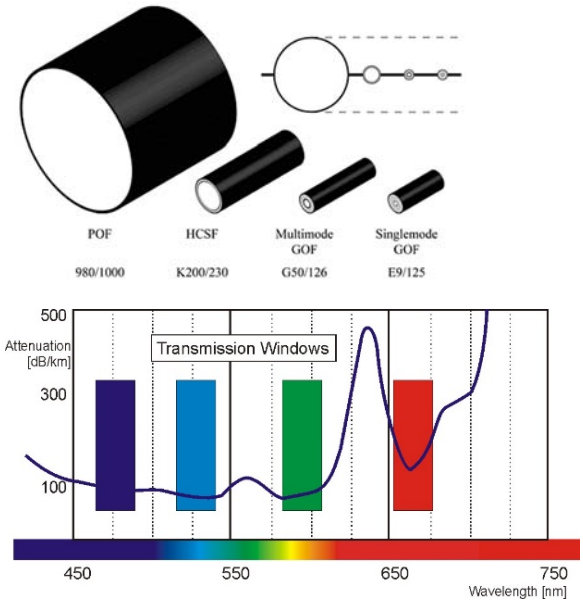

Fig. 1. Principle and attenuation of POF in the visible range [1].

1.2. The Motivation for WDM over POF

POF offers advantages compared to the established technologies. This leads to a broad usability in different sectors, such as the automotive, the in-house or the industrial sectors. This kind of fiber can also be applied for aviation or the medical sector. All these applications have one thing in common – they all need high-speed communication systems [4-7].

The standard communication over POF uses only one single channel [1, 2]. To increase bandwidth for this technology the only possibility is to increase the data rate, which lowers the signal-to-noise ratio and therefore only can be improved in small limitations.

This paper presents a possibility to open up this bottleneck. In glass fiber technology, the use of the WDM (wavelength division multiplexing) in the infrared range at about 1550 nm has long been established [8-10]. This multiplexing technology uses multiple wavelengths to carry information over a single fiber [11]. This basic concept can – in theory – also be assigned to POF. However POF shows different attenuation behavior, see Fig. 1. For this reason, only the visible spectrum can be applied when using POF for communication.

For WDM, two key-elements are indispensable: a multiplexer and a demultiplexer. The multiplexer is placed before the single fiber to integrate every wavelength to a single waveguide. The second element, the demultiplexer, is placed behind the fiber to regain every discrete wavelength. Therefore, the polychromatic light must be split in its monochromatic parts to regain the information. These two components are well known for infrared telecom systems, but must be re-developed for POF, because of the different transmission windows.

One technical solution for this problem is available [12], but it cannot be efficiently utilized in the POF application scenario described here, mostly because this solution is afflicted with high costs and therefore not applicable for any mass production.

2. Basic Concept of the Demultiplexer

As mentioned before, a demultiplexer is essential for WDM. Several preconditions must be fulfilled to create a functional demultiplexer for POF. First of all, the divergent light beam, which escapes the POF, must be focused. This is done by an on-axis mirror. In the first attempt, a spherical mirror is used. To get perfect results without any spherical aberrations, an ellipsoid mirror should be used.

The second function is the separation of the different transmitted wavelengths. In Fig. 2, this principle is illustrated for three wavelengths (red, green, blue). This is not a limitation for possible future developments, but rather an experimental basis from where to run the various simulations described below. The diffraction is done by a diffraction grating. The diffraction is split into different orders of diffraction. The first order is the important one to regain all information. There a detector line can be installed to detect the signals.

Because the grating is attached to a bended basement only one element can cover both functions, the focusing and the diffracting. The higher the grating constant g of the diffraction grating is the sharper are the maxima of the different diffraction orders. The diffracted light interfere positively on the detection layer for:

$$z\lambda = g(\sin\alpha + \sin\beta) \tag{1}$$

The resolution of the diffraction grating follows the Rayleigh Criterion and depends on the complete number of grating steps N and not on the grating constant:

$$\frac{\lambda}{\Delta\lambda} \leq zN \tag{2}$$

The light is also not afflicted with any aberrations or attenuations of a focusing lens or other refractive elements, which are necessary for any other setup [13, 14].

Another characteristic of key elements for POF communication is the three dimensional approach. Key elements of glass fiber communication are usually designed planar. This simplification cannot be adopted for POF communication, because of the large Numerical Aperture of the POF.

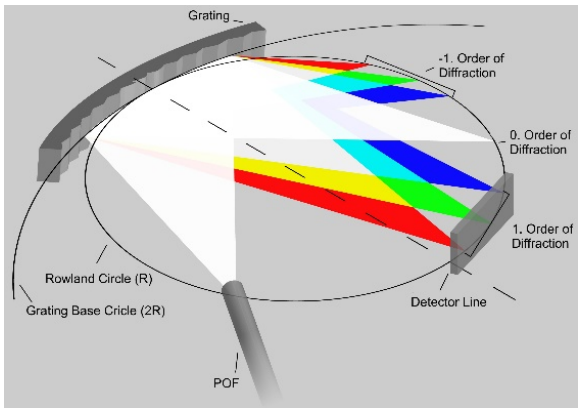

Fig. 2. Principle sketch of a Rowland spectrometer.

3. Results of the Simulation

In the following steps, an optical simulation software is used to design a demultiplexer based on the general concept outlined above. For the current task, the software OpTaLiX provides all required functionalities [15]. This approach offers different advantages: It is easy to design a setup and to analyze and to evaluate the simulated results. Furthermore, effective improvements of the configuration can be simulated quickly.

In Fig. 3, the 2D plot of the demultiplexer with an ellipsoid mirror and a grating is shown. The multicolored light, consisting of three wavelength (450, 520 and 650 nm) is emitted by a polymeric fiber. It hits the aspheric mirror, where it is focused and diffracted in its monochromatic parts. The light is focused onto a POF- or detector-array.

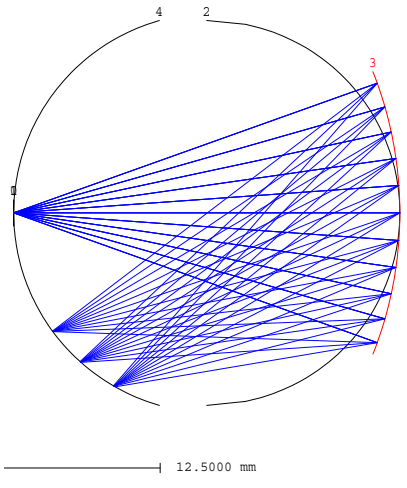

Fig. 3. 2D plot of the demultiplexer.

Without a grating, a perfect point to point mapping (without any aberrations) is possible with an ellipsoid mirror because of the two foci, but there is no separation of the different channels. With a grating stamped on the mirror, the separation of the multicolored light in its monochromatic parts is possible. But this grating distorts the optical path of light dramatically.

The first change is that the gap of the different colors in the image layer (here the POF- or detector array) increases with the line density of the grating. This can be noticed for an ellipsoid mirror and for a spherical mirror as well. The advantage of the spherical mirror is that the shape can be produced for injection molding easier. This optimization process was shown in different papers before [13, 16].

The result so far is that the demultiplexer can separate three colors with enough space between them to regain the information with a POF- or detector-array. The shapes of the foci feature low coupling losses and the shape of the mirror is producible in injection molding.

The mentioned results are satisfying for the optical requirements, but there are manufacturing requirements of this device as well. However, the line density of 1200 l/mm for the first diffraction order is too high for mass production. The goal is to produce a key component for high-speed POF communication for a reasonable price. The structure size of the grating is very small. To solve this problem, higher diffraction orders can be used, meaning that the second and the third order will be researched further on.

3.1. Grating Efficiency for Different Diffraction Orders

Focusing of the light is one part of the setup. The other task is separating the different wavelengths. Both of them is done by a dispersion grating based on an aspheric mirror. This grating can only be optimized for one diffraction order. A simple linear grating guides most of the light into the first diffraction order. But to reduce the line density of the grating for better manufacturing possibilities a higher order (second or third) should be used instead. Therefore a blazed grating must be applied. This Littrow configuration optimizes the light guidance in a higher diffraction order. But this kind of grating can only be improved to nearly 100 % for a single wavelength. It is common to use a green peak wavelength for the whole visible spectrum to get the best efficiency. The result of this optimization of the grating is shown in Fig. 4 for the first, the second and the third diffraction order.

The first order of diffraction exhibits the best efficiency. The value is above 60 % for the complete visible spectrum, but is not applicable in our case due to problems with the fabrication. The second order of diffraction offers more than 40 % of efficiency in the range from 450 nm to 650 nm. The third order has two maxima: at 470 nm and 630 nm to cover a larger

wavelength range, but the efficiency is not higher than 50 %. That means 3 dB of the power will be lost just for the grating. This is too much for the insertion loss of this component. Consequently the second order seems to be the only suitable order of diffraction. This is not the only reason for the use of the second order. Third and higher orders will be overlapped in the visible region by lower orders and this will cause crosstalk.

3.2. Examination of Image Layer for the Blazed Grating

The shape of the foci in the detection layer will not be changed dramatically by optimizing the grating. The higher the line density the larger is the gap between the colors. But this will also lead to greater aberrations. Therefore, it is easy to find the right line density for the grating. The line density of the grating must be high enough to separate every color in the image layer. So the distance must be at least 0.5 mm between the blue and the green focus point and also between the green and the red focus point. Higher line densities would lead to greater aberrations and to more problems in the fabrication process. The image layer for the second order of diffraction and a line density of 500 l/mm is shown in Fig. 5 and Fig. 6. As can be seen, this parameters fit well to the requirement. An additional fourth color with a wavelength of 405 nm is added. Also the radii in the x- and y-axis are optimized to suppress the astigmatism caused by the Rowland spectrometer setup.

This works well in one direction but in the other direction the astigmatism will remain even for the optimized setup.

The spot diagram can only give a hint of the real size of the focus points, because the rays were sent through the optical systems by an ideal source. But in the setup the source will be a POF, with a core diameter of 0.98 mm. This will lead to larger focus points. To get a realistic estimation, the simulation is enhanced to an area light source with a diameter of 0.98 mm. The result can be seen in Fig. 7.

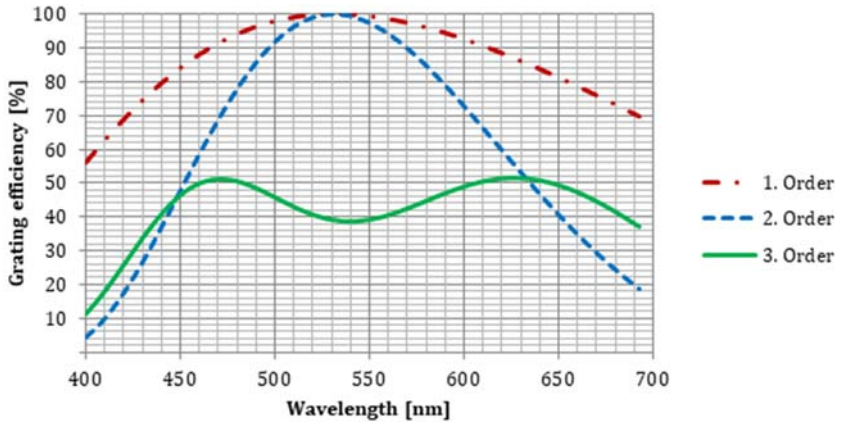

Fig. 4. Grating efficiency for different diffraction orders.

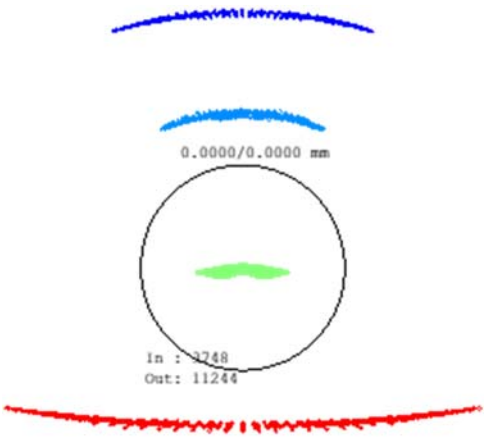

Fig. 5. Spot diagram
(not optimized, circle diameter 1 mm).

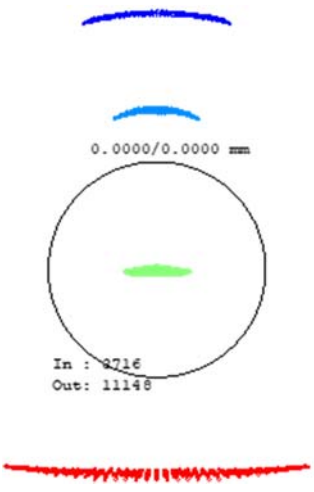

Fig. 6. Spot diagram
(optimized, circle diameter 1 mm).

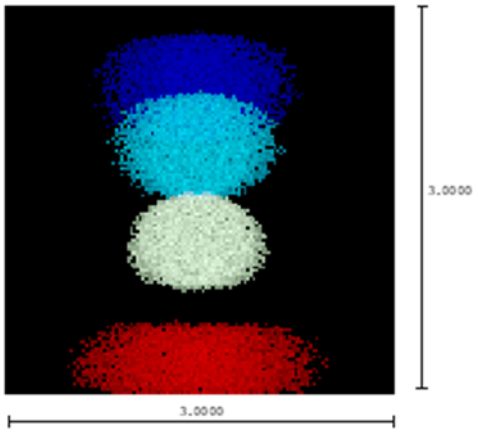

Fig. 7. Image layer of the setup for an area light source.

4. Production of a Prototype

After the design for the DEMUX prototype has been created, the steps for making the prototypes are explained below. Due to the complexity of the spherical grid structure to be created, it was necessary to commission a competent partner for the production of the DEMUX prototypes. The manufacture of the DEMUX prototypes took place in close cooperation with a manufacturer of precision injection molding tools and parts. These have the necessary equipment to create microstructures using ultra-precision machining in injection molding tools.

The grid consists of 4078 lines on the toric surface. This requires too much memory, which caused the program to crash. The following approaches to solving this problem have been worked out.

A first approach is to divide the grid into several sections. It turned out that with 11 sections it is possible to create the lattice structures in SolidWorks. The division into grid sections was previously discussed with the manufacturing company and classified as feasible. The 3D data can be read into the software of the machine and processed. Section 6 of 11 can be seen in Fig. 8. The individual sections are converted into CAM data in the machine and then run through section by section.

The first prototype produced using this method did not have a homogeneous lattice. There were height differences between the grid sections. These are due to the section-by-section CAD data, as the machine has to stop for each section and start again. The machine-related tolerance when approaching the workpiece with the diamond tool results in variances in the height of the various sections. This showed that this type of CAD data processing is unsuitable for high-precision microstructures.

Another approach can be found with which it is possible to manufacture the entire grid without having to remove the diamond tool.

Another approach was developed in collaboration with Wodak. Using a special CAM (computer-aided manufacturing) program called Di sys, grid surfaces can be described. The program has been specially developed for use in ultra-precision machines. It creates optical surfaces that can be produced with CNC machines. It was originally developed for the production of aspherical, diffractive, Fresnel and hybrid, circularly symmetrical optics.

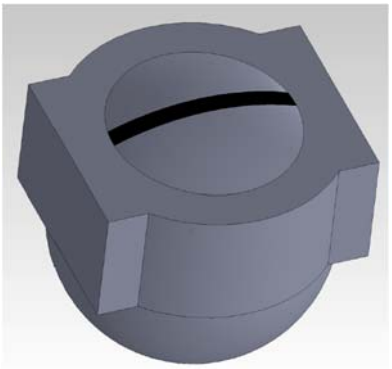

Fig. 8. CAD model of the 6th grid section of a total of 11.

The grid of the DEMUX is not circularly symmetrical on the toric surface. In cooperation with the manufacturer of Di sys, the CAM software was expanded to create non-circularly symmetrical optics. For this, a section through the grid must be available as a drawing or CAD data. Since the strength of SolidWorks lies in the 3D area, it has fewer functions than other programs in the creation of 2D drawings. That is why the 2D section of the grid was created with the AutoCAD software. This CAD software was primarily developed for the creation of technical 2D drawings, which has been expanded over time to include the modeling of 3D objects [17].

AutoCAD has good tools for replicating structures, which also makes it the preferred software for creating masks for the semiconductor industry. With this and the fact that AutoCAD is a vector drawing program, it is possible to model the section through the grid. Fig. 9 shows an excerpt from the drawing.

Ultra-precision machining is used to manufacture the prototypes. This is done by the company. The processing took place on the Freeform 700a from AMETEK Precitech Inc. The prototype is made from a PMMA blank.

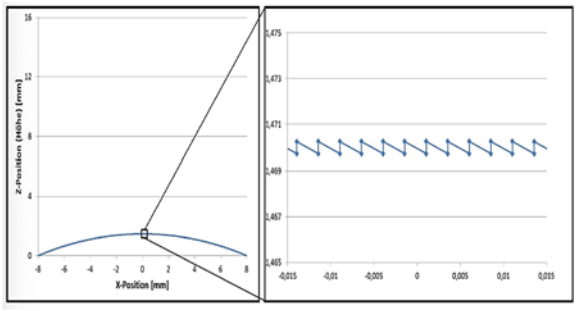

Fig. 9. Section of the DEMUX grid based on the AutoCAD drawing; left: entire grid; right: enlarged section.

The individual process steps are explained below:

1. The hemisphere and rectangular structure are milled out of a PMMA rod blank. A lead is left on the hemisphere surface for later UP machining.

2. The rod is then sawn off at the point where the surface for the grid is to be created (with enough overhang to create the toric grid).

3. The surface on which the grid will later be created is faced on the UPB machine.

4. The workpiece is attached to the flat surface created (vacuum suction). The hemispherical surface is turned to optical surface quality with a diamond tool and receives the designed final dimensions.

5. The hemisphere is sucked in with a device so that the grid processing can take place on the opposite side.

6. Now the best-fit preform of the toric surface of the grid is created.

7. The sawtooth structure of the grid is then cut with a special diamond tool (so-called ripping of the grid contour).

The grid processing is the most difficult and time-consuming production step. As shown in Fig. 10, the contour of each saw tooth is traversed several times with the diamond tool (ripping).

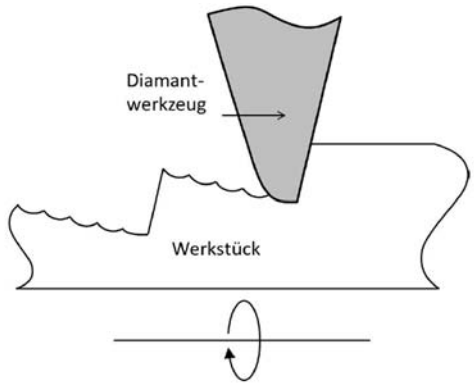

Fig. 10. Principle of the grid lines production by marking off the sawtooth structures (adapted from [18]).

A special diamond is used, which has a 2 mm radius at the tip and is halved in the middle. The feed rate, the speed at which the grid lines are cut, was 300-400 mm/min. The lateral infeed describes how much the diamond tool advances with each cutting (also known as the feed rate). The lateral infeed is 0.2-0.3 µm. All parameters are summarized in Table 1.

Table 1. UPB processing parameters.

Parameter	Value
Feed v_f = [mm = min]	300
Infeed f_z = [µm]	0.2
Number of grid lines N	4078
Length of the grid line l_g [mm]	10.195
Lattice constant [µm]	2.5

During machining, the diamond tool remains fixed and only the workpiece is moved. The structure of the grid with the axes is followed line by line. The toric surface shape of the grid can be approached through the free control of three axes. Using the parameters from Table 1, the processing time for the entire grid can be calculated as follows:

$$t_{bearb} \approx \frac{\pi}{4} * \frac{l_g N d}{f_z v_f} = 22,68h \qquad (3)$$

Since it is not a square area, but approximately describes a circular area, the result must be multiplied by the factor pi/4 for conversion. It took almost 23 hours to process the grid. This harbors risks such as breakage or wear of the diamond tool during the processing time and places high demands on the process stability. By marking the structure with the diamond tip, a periodic one is created roughness. Eq. (4) gives a theoretical value for the roughness depth of:

$$R_t = \frac{f_z^2}{8 r_{wz}} = \frac{(0,2\mu m)^2}{8 \cdot 2\mu m} = 2,5nm \qquad (4)$$

After the prototype has been produced, the grille is coated with aluminum. The aluminum coating increases the re ectivity in the visible spectrum (VIS) [19, 20]. This is necessary to ensure the functionality of the grid. Without the re ecting layer, a large part of the Light power transmitted at the interface of the grating. The blaze angle of the grating is 11.97°, which means that the incident light beam hits the interface between PMMA and air at this angle.

A refraction angle of β=18° follows from Eq. (1). With the angle of refraction and the Fresnel Eq. (5), the degree of reflection can be determined:

$$\begin{aligned} r_{\perp}^2 &= -\frac{\sin(\alpha-\beta)}{\sin(\alpha+\beta)} = 4,42\% \\ r_{\parallel}^2 &= \frac{\tan(\alpha-\beta)}{\tan(\alpha+\beta)} = 3,35\% \\ R &= \frac{r_{\parallel}^2 + r_{\perp}^2}{2} = 3,89\% \end{aligned} \qquad (5)$$

Only 3.9 % of the input power is reflected by the grid. The demultiplexer would not work without a coating. The aluminum coating also allows the grid structure to be analyzed in a scanning electron microscope (SEM). A conductive surface is required for analysis in the SEM. Without this conductive layer, the surface would be charged in the SEM.

Furthermore, the layer protects against radiation damage and increases the number of secondary electrons, which leads to a better

Signal-to-noise ratio lead. [21, 22]. The coating was carried out using the PVD process (physical vapor deposition) in the clean room of the Institute for Micro and Sensor Systems (IMOS). The surface of the DEMUX grid was coated with the LS500ES PVD

system from Ardenne Anlagentechnik, GmbH. It is a magnetron sputtering system. In the magnetron sputtering process, a magnetic field-enhanced plasma discharge is generated in a chamber filled with argon. The chamber is evacuated with a residual pressure of 10E-1-10E-2 Pa (high vacuum). The plasma is generated by a high DC voltage, which is applied between the target (coating material) and the substrate (component to be coated). Positively charged argon ions are accelerated from the plasma to the target by the DC voltage field.

The impact of the ions on the target results in an impulse transmission, followed by a collision cascade. Particles of the target are knocked out, which are deposited on the substrate and form a thin layer. In order for the particles to reach the substrate without colliding with other particles, the mean free path must be greater than the distance between target and substrate, which is achieved by evacuating the chamber. With a pressure of 10E-1-10E-2 Pa, a mean free path of approx. 6 to 60 cm can be set.

The sputtering process is particularly suitable for coating the plastic components, as the process does not require additional heating of the substrate, which is crucial for plastics [23]. Nevertheless, the chamber is heated by the energetic collision processes in the plasma and on the target. It is therefore necessary to apply the layer gradually so that the temperature does not rise above the glass transition temperature of the plastic.

Before the coating is carried out, there is a cleaning step in the PVD system. The surface is bombarded with argon ions from the generated plasma. This has no negative effects on the optical properties of the DEMUX, as it only takes a very short process time (<1 min). Analyzes have shown that there is no deterioration in the transmission properties due to increased scattered light [23].

To prevent the plastic in the chamber from being overheated, controlled cooling phases have been integrated into the process flow. From the deposition rate (which was determined from numerous coatings of the IMOS) and the 2 times 30 seconds process time, a layer with about 115 nm was produced. The result can be seen in Fig. 11(b).

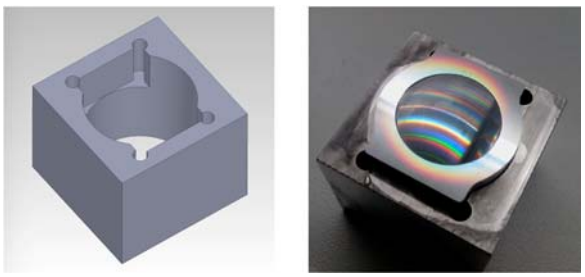

Fig. 11. a) Holder for the sputtering process;
b) DEMUX in the holder with aluminum coating.

The layer does not offer adequate protection against damage, as it is too thin at approx. 100 nm [24]. Therefore extreme caution is required when handling the prototypes. One advantage of the coating is the ability to create a master for the injection mold. The electrically conductive aluminum layer is used for an electroplating process. This creates a negative impression, which serves as a mold insert for the injection molding of replications.

5. Conclusion

The Polymer Optical Fiber exhibits many advantages in comparison to glass fiber and copper for short-howl communication.

State of the art for POF communication is the use of only one single channel. This means a limitation of bandwidth. The solution for this bottleneck is WDM over POF, where not only one channel is used to transmit the information over a single fiber. To use this technique, two key elements: a multiplexer and a demultiplexer have to be designed completely new, because already established key elements for WDM communication over glass fiber in the infrared range cannot be applied.

The simulation results show that it is possible to build up a demultiplexer by means of a Rowland spectrometer. A special shape of the mirror is needed to suppress most of the aberrations, which results from the grating. The improved demultiplexer can separate three colors without any overlap. But for four colors this setup will gain high crosstalk (Fig. 7). Therefore, the basic idea of focusing the light with different wavelength by means of adjusting the two radii should be reconsidered. Besides increasing the line density an alternative could be the use of a holographic grating. But this will lead to higher production costs. The grating efficiency for the second order of diffraction is suitable for source in the range of 450 nm to 650 nm and the setup can also be used as a spectrometer in the visible wavelength range.

References

[1]. Daum W., Krauser J., Zamzow P. E., Ziemann O., POF – Polymer Optical Fibers for Data Communication, *Springer-Verlag*, Heidelberg, 2002.
[2]. Nalwa H. S., Polymer Optical Fibers, *American Scientific Publishers*, California, 2004.
[3]. Marcou J., Plastic Optical Fibres – Practical Applications, *John Wiley & Sons, Masson*, 1997.
[4]. Brandrup J., Immergut E. H., Grulke E. A., Polymer Handbook, *Wiley-Interscience*, 1999.
[5]. Infineon Technologies AG, Infineon Technologies, (http://www.infineon.com/de/), 2008.
[6]. Kragl H., A product family for simplex POF home networks, (http://www.pofac.de/itg/fg_5_4_1/de/fachgruppentreffen/treffen21.php), 2006.
[7]. Chen R. T., Lipscomb G. F., WDM and Photonic Switching Devices for Network Applications, *Proceedings of SPIE 3949*, 2000.

[8]. Colachino J., Mux/DeMux Optical Specifications and Measurements, *Lightchip, Inc. White Paper, Lightreading*, 2001.
[9]. Gnauck A. H., Chraplyvy A. R., Tkach R. W., Zyskind J. L., Sulhoff J. W., Lucero A. J., *et al*., One terabit/s transmission experiment, in *Proceedings of the Optical Fiber Communication Conference (OFC'96)*, 1996.
[10]. Batchellor C. R., Debney B. T., Thorley A. M., Swanenburg T. J. B., Heydt G., Auracher F., *et al.*, A coherent multichannel demonstrator, *Electr. & Comm. Engineer. J.*, 1992, pp. 235-242.
[11]. Voges E., Petermann K., Optische Kommunikationstechnik, *Springer-Verlag*, Heidelberg, 2002.
[12]. Fraunhofer Institute for Integrated Circuits, Optical multiplexer for short range communication, (http://www.iis.fraunhofer.de/ec/oc/download/demux.pdf), 2008.
[13]. Fischer U. H. P., Haupt M., Optical development steps of a fully integrated miniature spectrometer designed for injection molding fabrication, in *Proceedings of the 3d International Conference on* Optics, *Photonics and Lasers (OPAL'2020)*, Tenerife, Spain, 21-23 October 2020, pp. 44-48.
[14]. Last A., Mohr J., Fehllicht in LIGA-Mikrospektrometern, *Forschungszentrum Karlsruhe Wiss. Berichte*, 2003.
[15]. Blechinger H., OpTaliX: Optical Design Software, (http://www.optenso.com), 2012.
[16]. Fischer U. H. P., Haupt M., Advanced integrated WDM System for POF Communication, *SPIE Photonics West*, 2009.
[17]. Autodesk, Autodesk Homepage, 2013.
[18]. Fleming M. B., Hutley M. C., Blazed diffractive optics, *Applied Optics*, Vol. 36, Issue 20, 1997, pp. 4635-4643.
[19]. Hass G., Waylonis J. E., Optical constants and reflectance and transmittance of evaporated Aluminium in the Visible and Ultraviolet, *Journal of the Optical Society of America*, Vol. 51, Issue 7, 1961, pp. 719-722.
[20]. Morton R. G., Blasiak T. C., Reflective overcoat for replicated diffraction gratings, *Spectronic Instruments, Inc.*, 1999.
[21]. Sawyer L. C., Grubb D. T., Polymer Microscopy, *Springer*, 2008.
[22]. Höflinger G., Brief Introduction to Coating Technology for Electron Microscopy, (http://www.leica-microsystems.com/science-lab/briefintroduction-to-coating-technology-for-electron-microscopy/).
[23]. Bäumer S., Bauer T., Marschall D., Handbook of Plastic Optics, *Wiley-VCH Verlag*, 2010.
[24]. Palmer C., Diffraction Grating Handbook, *Newport Corporation*, Vol. 46, 2005.